sustainability

MDPI

Article

Influence of Mineral Deposition on the Retention of Potentially Hazardous Elements in Geothermal Hot Spring Sediments

Yafeng Wang and Hefa Cheng *

MOE Key Laboratory for Earth Surface Processes, College of Urban and Environmental Sciences, Peking University, Beijing 100871, China

* Correspondence: hefac@umich.edu; Tel.: (+86) 10 6276 1070

Abstract: Geothermal hot springs are known to contain lots of potentially hazardous elements (PHEs) which may threaten human health. Their release on Earth's surface is greatly dependent on the retention of the sediments at the spring outflux. In this study, the hot spring waters and the sediments at the corresponding sites were collected from the Nagqu geothermal field on the Tibetan Plateau. The water geochemistry and sediment mineralogy were analyzed using inductively coupled plasma mass spectrometry (ICP-MS), X-ray fluorescence (XRF), and X-ray diffraction (XRD). The association of the PHEs with minerals was analyzed. The results indicated that the Nagqu hot springs did not show highly elevated PHE concentrations, but Be, As, and Tl in some hot springs exceeded the class Ⅲ groundwater limit of China by up to 2, 2, and 19 times, respectively. Cs had a relatively high concentration, of up to 776 μg/L. As, Co, Se, Tl, and U were probably captured by Fe sulfide in the sediments. Carbonate minerals had a strong retention to Be and Cs. Clay minerals showed apparent affinity for V and Cr. The immobility of PHEs from the geothermal hot spring source is controlled by the deposition of minerals at the spring vent.

Keywords: geothermal spring; potentially hazardous elements; environmental impacts; mineral precipitation; association

1. Introduction

As a clean and renewable energy, the geothermal hot springs, which are mainly distributed in areas with active geological and structural activities [1, 2], are widely developed for power generation and directly used for bathing by the local residents [3]. However, with the energy demand increasing, lots of environmental and health concerns emerged along with the development of geothermal energy [4, 5]. Because of the contacts with geological formations overlying the reservoir and the input of the volatile matter from the magma, the hot spring water was polluted by lots of hazardous and toxic matter [6-12]. The release of the hazardous and toxic components, such as heavy metals and hydrogen sulfide, from the geothermal springs could result in surrounding environmental contamination [5, 13], for example, polluting the river, drinking water, soil, and crops [14-17]. Potentially hazardous elements (PHEs) including heavy metals from the geothermal springs deserves attention because exposure to those harmful chemicals through water and food consumption probably lead to human health issues [18-24].

The portioning of the dissolved PHEs in surface environment is geochemically and mineralogically controlled. The declined temperature and pressure on Earth's surface result in the release of those pollutants which were dissolved in the hot spring water as various forms [25]. The PHEs from the geothermal sources are mainly discharged into the

Citation: To be added by editorial staff during production.

Academic Editor: Firstname Lastname

Received: date
Revised: date
Accepted: date
Published: date

environment while some fractions of them are retained by the hot spring precipitates. In the underground geothermal systems, the inorganic elements such as Ca and Si are dissolved under the high temperature and high pressure environment [26]. Those chemical elements of elevated concentrations precipitate to form sediment and sinter when the hot spring water is discharged to the Earth surface and the equilibrium conditions change [26-28]. The hydrothermal carbonate deposits travertines often form at the geothermal sites due to the CO_2 degassing [29-31]. Siliceous sinters such as opaline silica deposit also often form at the geothermal sites [32, 33]. The transfer of chemical elements from the hot spring water to the sediment is a key process influencing the release of the hot spring source elements to surface environment [34]. Some elements such as As, Sb, and Hg can be trapped by the geothermal spring sinters or enriched in the geothermal spring sediments [35, 36]. W was demonstrated to be enriched in the hot spring sediment with high Fe content [37]. As concentration in the hot spring sediments from the north-central Andean region of Ecuador reached 717.6 mg/kg [38]. The capacity of the PHEs discharged into the surrounding environment of the hot springs is greatly dependent on the retention of the sediment at the spring vents.

In China, the geothermal hot springs are mainly distributed in the Yunnan-Sichuan-Tibet Geothermal Province [39]. The previous research indicated that the PHEs from the geothermal hot springs have caused environmental pollution in Tibet [40-42]. In particular, As showed the most widely and sever among all the hot spring source hazardous elements [40]. The mineralogy and geochemistry of the geothermal deposits were largely studied. However, the retention characteristics of the hydrothermal deposits on the PHEs at the geothermal hot spring sites are scarce. In this study, the association of the minerals and the PHEs in the hot spring sediments were analyzed, which will help to understand the controlling factors of the PHEs immobility in the surface environment.

2. Materials and Methods

Twelve hot spring waters and the corresponding surface sediments (**Figure 1**A) were collected in a geothermal field in Nagqu on the Tibetan Plateau, China. Three hot spring sinters (**Figure 1**B) were sampled for the comparison with the sediments at the abandoned hot spring pipes. The water pH was measured using an electronic pH meter and the temperature was measured using a mercury thermometer. The water samples were filtered in-situ using 0.22 μm syringe filter to remove the suspended particles. The water samples were acidified to pH < 2 and preserved at 4 ℃ before chemical analysis. The sediments and sinters were air dried in the laboratory and then ground to pass a 200-mesh sieve for chemical analysis. Accurately weighted sediment and sinter samples (0.2 g) were digested with a mixture of 9 mL HNO_3 and 3 mL HF in a microwave digestion system following Method 3052 of the United States Environmental Protection Agency (USEPA). The concentrations of the PHEs in the hot spring waters and the digestion solutions of the sediments and sinters were determined using inductively coupled plasma mass spectrometry (ICP-MS). The major and minor element contents of the sediments and the sinters were measured using X-ray fluorescence (XRF). The mineral phases in the solid samples were identified by X-ray diffraction (XRD).

Figure 1. Sampling sites of hot spring waters, sediments, and sinters in the Nagqu geothermal field. (A) hot spring-vent on Earth's surface; (B) abandoned hot spring pipe in the geothermal field.

3. Results and Discussion

3.1. Distributions of the PHEs in the hot spring water and sediments

The pH of the hot spring water is close to neutral with the average value of 7.3 (ranging from 6.7 to 8.2) (**Table 1**). The temperature range was 35.6–78.0 °C, covering low temperature springs, moderate temperature springs, and high temperature springs (>70 °C) [43, 44]. Fifteen potentially hazardous elements (Be, V, Cr, Mn, Co, Ni, Cu, Zn, As, Se, Cd, Cs, Tl, Pb, and U) were determined for the hot spring water samples and their concentration distributions are presented in **Figure 2**. Except for Cd which was under the instrumental detection limit in all hot spring water samples, another 14 elements were detected in various levels although U was only detected in 5 water samples. The data distributions of the PHEs in **Figure 2** shows that the concentrations of Cr, Cu, Zn, and Cs in the waters fluctuates in a small range, while other elements were distributed dispersedly in a wider range. In the standard for groundwater quality of China (GB/T 14848—2017), the total concentrations of Be, V, Cr, Mn, Co, Ni, Cu, Zn, As, Se, Cd, Cs, Tl, and Pb among the studied PHEs are regulated. The comparison to the standard shows that Be, As, and Tl exceeded the class III groundwater quality as high as 2, 2, and 19 times, respectively. This indicated that those 3 elements have a potential to cause environmental and health issues if the geothermal spring water are consumed by the local residents.

Natural surface water and groundwater generally have low Cs concentration (for example, < 5 μg/L or < 1.0 μg/L) [45, 46] and Cs is not currently regulated for the groundwater quality in China. However, Cs had high concentrations in the Nagqu hot spring water. The average concentration of Cs in the water samples was 549 μg/L with the highest value

up to 776 μg/L. The high concentrations of Be, As, Cs, and Tl in the hot spring water has impacted their contents in the sediment. As shown in **Figure 3**, only the contents of Be, As, Cs, and Tl in the hot spring sediments exceeded their average levels in the Tibetan surface soils [47]. The As concentrations in the hot spring sediments varied from 1.6 to 717.6 μg/g [35, 36, 38]. Other studied PHEs were lower than the soil background values or at the equivalent level. The comparison shows that most of the PHEs had higher concentrations in the sediments than in the sinters and only the Be concentration in the sediments were lower. The geoaccumulation index (I_{geo}) calculated according to equation (1) [48]:

$$I_{geo} = log_2(\frac{C_n}{1.5 \times B_n}) \quad (1)$$

where C_n is the concentration of the element n in the sediment sample, in μg/g; B_n is the background value of the element n in Tibetan surface soil, in μg/g. The pollution level of soil is classified into 7 categories based on the calculated I_{geo} : 1) $I_{geo} \leqslant 0$ (practically uncontaminated); 2) $0 < I_{geo} \leqslant 1$ (uncontaminated to moderately contaminated); 3) $1 < I_{geo} \leqslant 2$ (moderately contaminated); 4) $2 < I_{geo} \leqslant 3$ (moderately to heavily polluted); 5) $3 < I_{geo} \leqslant 4$ (heavily contaminated); 6) $4 < I_{geo} \leqslant 5$ (heavily to extremely polluted); and 7) $I_{geo} > 5$ (extremely contaminated).

The calculated I_{geo} (**Figure 4**) suggested that the studied PHEs did not pollute the sediments in most cases. The sediments were heavily and extremely contaminated by Tl in some cases. Only one sediment showed heavily contaminated by As. However, the heaviest contamination cause by As and Tl occurred on the same sediment sample and most of the sediments were uncontaminated or moderately contaminated. The average I_{geo} indicated that the hot spring sediments in the Nagqu geotherm field were moderately contaminated by Tl.

Table 1. pH and temperature of the hot spring water samples.

Sample	pH	Temperature (℃)
Water 1	8.0	78.0
Water 2	7.8	46.0
Water 3	6.7	40.0
Water 4	6.7	44.0
Water 5	7.6	40.0
Water 6	7.1	39.4
Water 7	7.4	37.0
Water 8	7.2	40.6
Water 9	7.0	35.6
Water 10	7.4	58.2
Water 11	8.2	63.8
Water 12	7.0	53.0

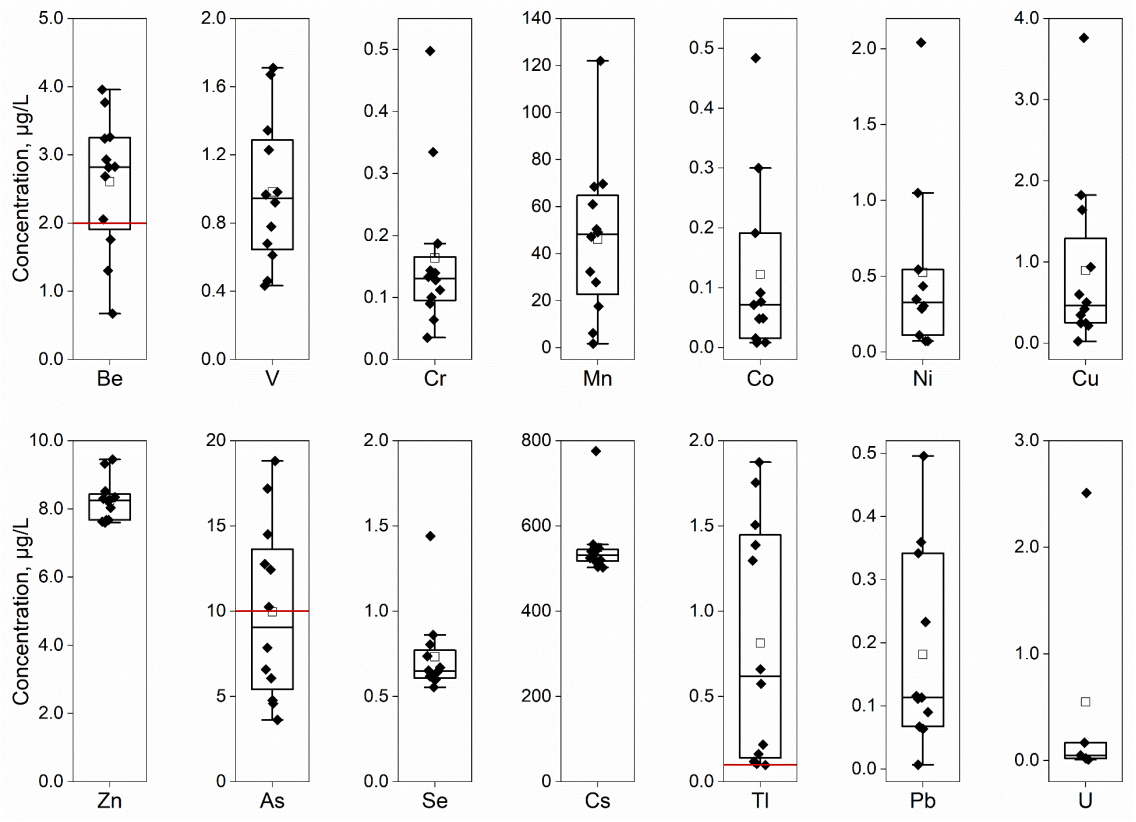

Figure 2. Concentrations of the potentially hazardous elements in the geothermal hot springs from Nagqu on the Tibetan Plateau, China. (Red lines represent the contaminant limits for class III groundwater in China, Be ≤ 2 μg/L, As ≤ 10 μg/L, Tl ≤ 0.1 μg/L).

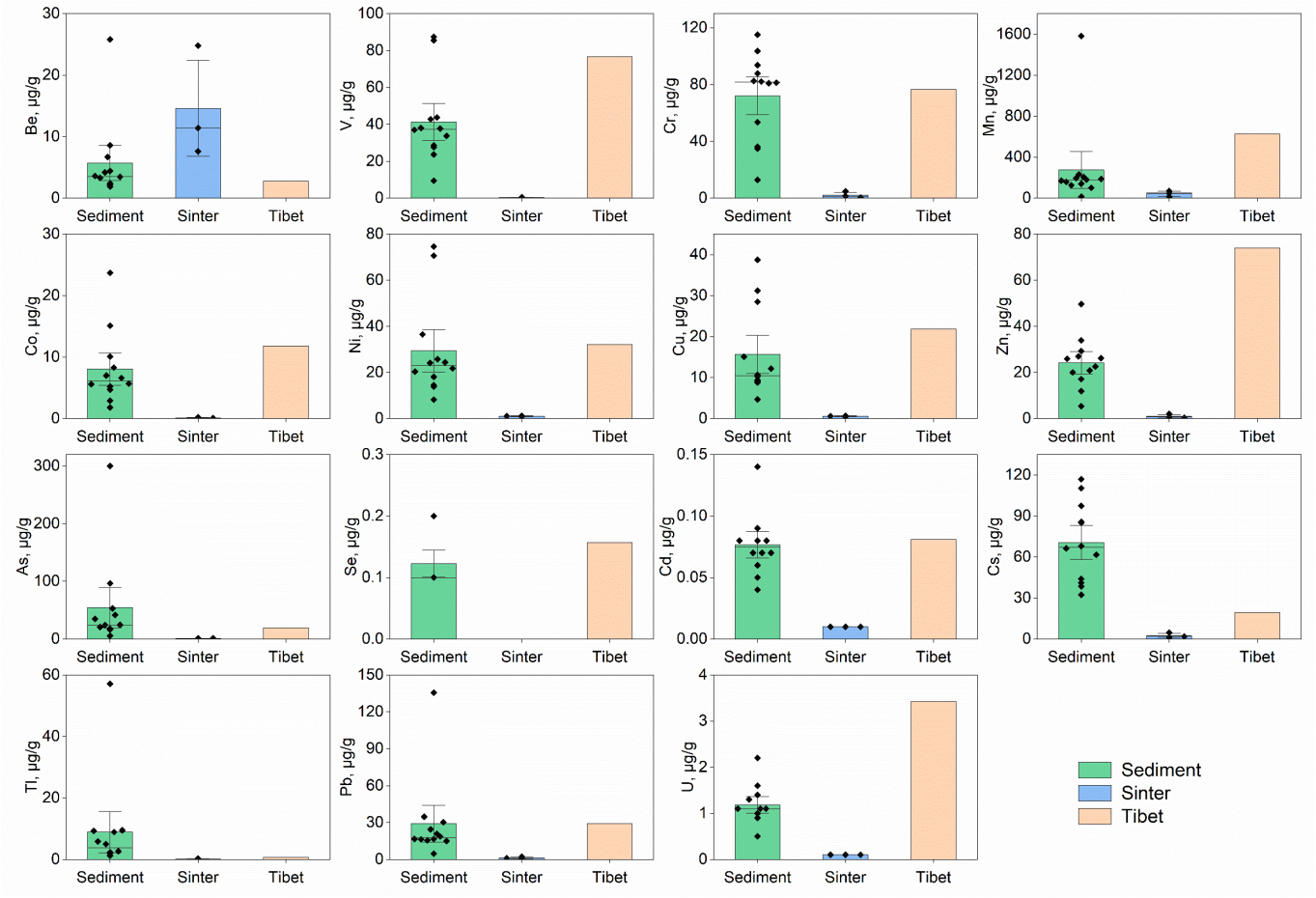

Figure 3. Concentrations of the potentially hazardous elements in the hot spring sediments and sinters and a comparison to their average levels in the Tibetan surface soils.

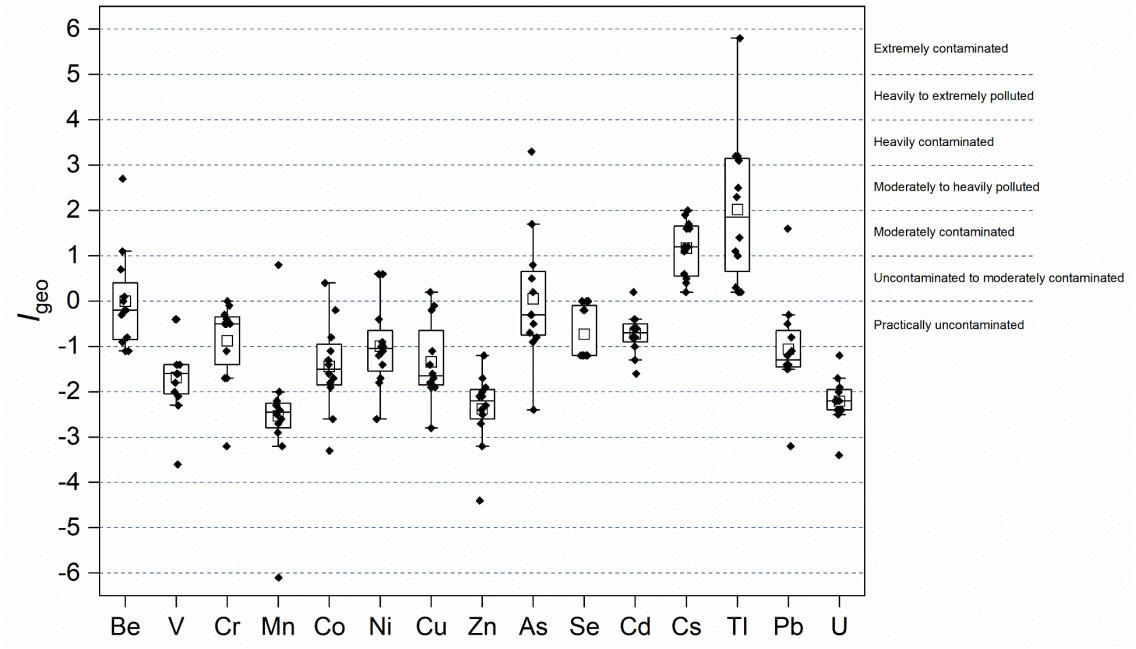

Figure 4. The I_{geo} of the potentially hazardous elements in the hot spring sediments.

3.2. Mineral compositions of the hot spring sediments

The major and minor element compositions of the Nagqu hot springs are reported in **Table 2**. The sediments were mainly composed of Ca and Si, with the total fractions ranging from 61%–85% (mean = 77%). The fraction of Ca+Si+Al was up to 93% and the average value was 84%. The major element compositions of the sinter were simpler than the sediments. Over 90% of the compositions were Si and followed by Sr accounting for low proportions (3.4%–5.1%). The relationship between the major and minor elements probably suggests the occurrence of minerals. The major and minor elements of the sediments can be classified into 3 groups: 1) Ca-Sr-Na-Mg, 2) Si-Al-K-Ti-P, and 3) Fe-S-Ba according to their Pearson correlation coefficients (**Table 3**). The elemental association indicated that the possible mineral compositions. For example, the solid phases with strong positive Si-Al correlation commonly represent the occurrence of clay minerals. Mg had a positive correlation with Ca, which possibly indicated that the dolomite was present in the sediments although it was not detected by XRD [31].

Table 2. Major and minor element compositions of the hot spring sediments and sinters (%).

Sample	CaO	SiO_2	Al_2O_3	Fe_2O_3	K_2O	Na_2O	MgO	SrO	TiO_2	BaO	SO_3	P_2O_5
Sediment 1	61.0	24.0	2.2	4.1	0.62	0.88	2.56	2.58	0.28	1.25	0.50	0.05
Sediment 2	10.3	66.3	6.3	6.2	3.30	0.79	0.59	0.20	0.85	0.60	4.51	0.14
Sediment 3	8.7	65.3	7.0	8.0	3.42	0.77	0.75	0.16	1.06	0.51	4.23	0.09
Sediment 4	0.4	78.0	10.3	5.4	3.54	0.18	0.51	0.01	0.77	0.12	0.68	0.11
Sediment 5	2.5	75.1	8.1	5.7	3.77	0.84	0.64	0.07	0.91	0.16	2.03	0.16
Sediment 6	1.8	76.6	7.9	5.1	3.36	0.68	0.48	0.07	1.19	0.25	2.49	0.14
Sediment 7	2.2	74.9	6.7	7.1	2.48	0.42	0.39	0.06	0.85	1.17	3.71	0.07
Sediment 8	1.3	60.0	6.1	14.0	2.39	0.49	0.00	0.06	0.82	2.88	11.75	0.11
Sediment 9	0.2	83.7	8.8	1.4	3.47	0.18	0.34	0.01	0.82	0.16	0.95	0.04
Sediment 10	10.2	65.6	9.1	6.8	3.20	1.11	1.00	0.17	1.05	1.05	0.53	0.14
Sediment 11	52.5	26.9	4.3	8.2	1.42	0.87	0.68	2.05	0.66	2.06	0.38	0.09
Sediment 12	33.8	40.2	8.9	8.4	2.62	0.95	1.08	0.93	1.04	1.36	0.52	0.19
Sinter 1	91.4	0.9	0.5	0.9	0.04	0.37	1.69	3.44	0	0.68	0.10	0.03
Sinter 2	92.2	0.7	0.1	0.9	0.04	0.62	0.32	4.10	0	0.81	0.08	0.04
Sinter 3	92.8	0.5	0.1	0.3	0	0.18	0.34	5.05	0	0.64	0.05	0.03

The minerals precipitated from the hot spring water is a kind of hydrothermal minerals. The mineralogical compositions of the hot spring sediments are generally heterogeneous and significantly correlated with spring pH [49]. Most of the collected Nagqu hot spring water samples had a pH slightly higher than 7.0 and the average pH value was 7.3 (**Table 1**). The near-neutral slightly alkaline environment of the springs is favorable for the formation of sinters and the crystallization of some minerals [26]. In this study, the mineral phases in the sediments and sinters were identified using XRD (**Figure 5**). As reported in **Table 4**, quartz was detected in all the sediment samples. Calcite, albite, and muscovite existed in most of the sediments. Aragonite identified in most of the sediments was the dominant feldspar mineral and orthoclase was detected in one sample. The mineral compositions of the sediments in Nagqu hot springs were generally simple. Compared to the sediments, the mineral phases identified in the sinter samples were fewer. The sinters can be defined as travertines because only carbonate minerals calcite and aragonite were identified by XRD [50-52]. Calcite and aragonite are the most common minerals

deposited from hot spring with the contribution of abiotic and biotic processes [28, 31, 50, 51, 53].

The calcite crystalized out of the hot spring water because of the decreasing temperature [54] and its precipitation happened after the precipitation of clay minerals whose formation through a gelatinous substance precursor [55]. Aragonite formed from spring water because of the rapid CO_2 degassing [28]. Clay minerals were abundant in hot spring sediments [56]. Ba in the sediments was supposed to be precipitated from the hot spring water as a form of barite ($BaSO_4$) due to the low solubility under lower temperature in the surface environment [54].

Table 3. Pearson correlation coefficients between the major elements of the hot spring sediments.

	CaO	**SiO_2**	**Al_2O_3**	**Fe_2O_3**	**K_2O**	**Na_2O**	**MgO**	**SrO**	**TiO_2**	**BaO**	**SO_3**	**P_2O_5**
CaO	1.00											
SiO_2	-0.96	1.00										
Al_2O_3	-0.71	**0.72****	1.00									
Fe_2O_3	-0.01	-0.26	-0.14	1.00								
K_2O	-0.86	**0.87****	**0.85****	-0.18	1.00							
Na_2O	**0.52***	-0.57	-0.31	0.20	-0.27	1.00						
MgO	**0.77****	-0.67	-0.53	-0.31	-0.62	**0.51***	1.00					
SrO	**0.99****	-0.93	-0.77	-0.06	-0.90	0.43	**0.77****	1.00				
TiO_2	-0.64	**0.57***	**0.70****	0.16	**0.76****	0.10	-0.58	-0.73	1.00			
BaO	0.40	-0.60	-0.50	**0.79****	-0.65	0.22	-0.01	0.39	-0.29	1.00		
SO_3	-0.40	0.18	-0.15	**0.73****	0.06	-0.21	-0.49	-0.37	0.12	**0.52***	1.00	
P_2O_5	-0.15	0.05	0.45	0.32	0.40	0.49	-0.15	-0.27	**0.60***	-0.05	0	1.00

Note: Underlined and bold digits represent a positive correlation for 12 determinations (*, $P < 0.05$; **, $P < 0.01$).

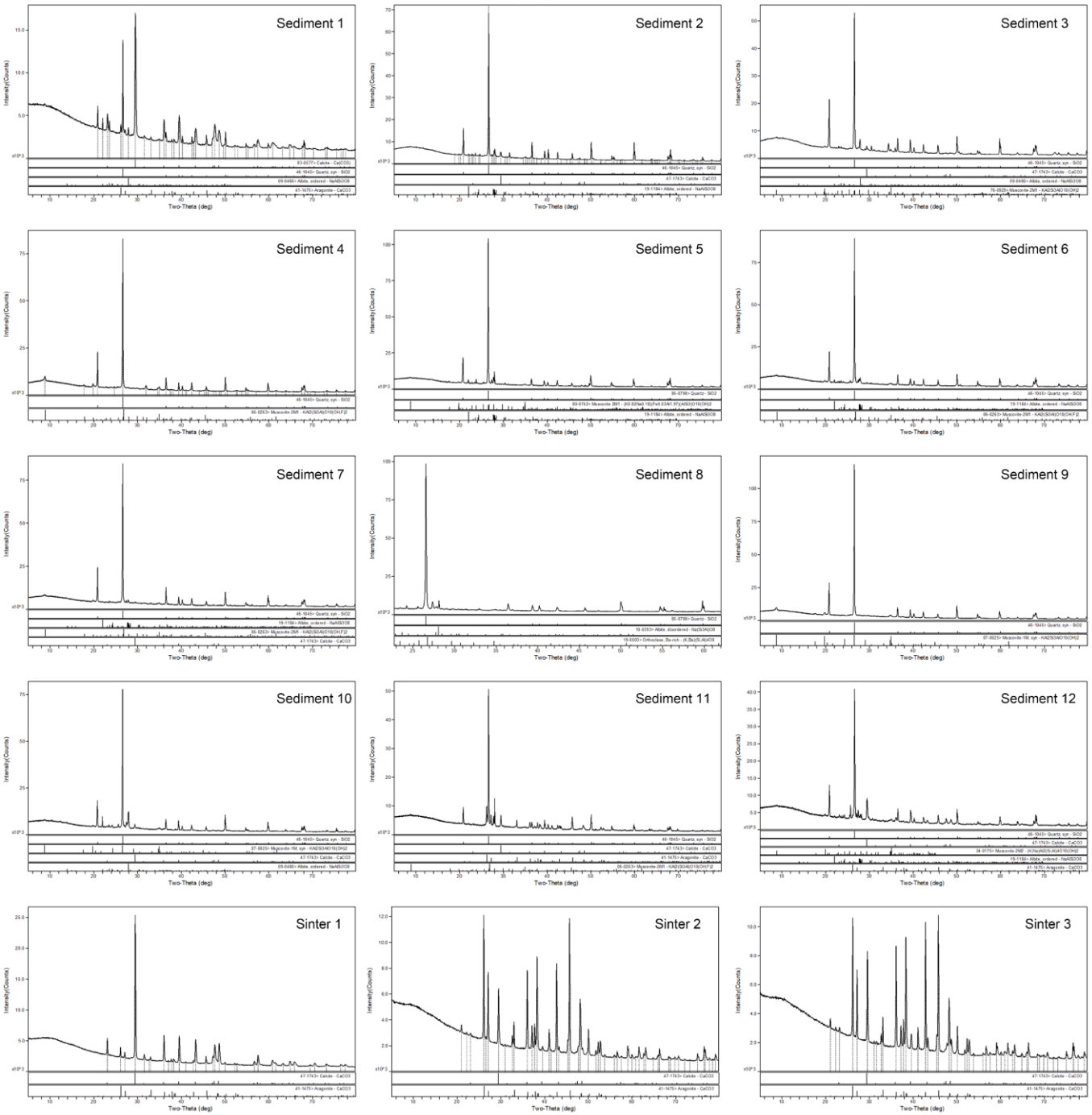

Figure 5. XRD patterns of the hot spring sediments and sinters.

3.3. Influence of mineral precipitation on PHEs immobility

The presence of minerals in the hot spring sediment has an important role in the retention of the potentially hazardous elements. For example, the enrichment of Sb in the hot spring sediments largely depends on the Fe abundance [39]. The Pearson correlation coefficients between all the studied PHEs and the major and minor elements are reported in **Table 5**. The correlations between Be, As, Cs, Tl and the major and minor elements are plotted in **Figure 6**. As shown in **Figure 6**A, Be was positively related with Ca and Mg. It suggested that Be in the hot spring sediments were mainly associated with Ca-bearing

minerals. Thus, the precipitation of calcite and aragonite probably captured the dissolved Be in the hot spring water. In addition, Be also showed a positive correlation with Sr (**Figure 6**A). The minerals containing Sr were not detected by XRD. However, Sr had a strong positive correlation with Ca in the hot spring sediments (**Table 3**), implying that it was probably a constituent of calcite and aragonite [58]. Thus, Be was supposed to be associated with calcite and aragonite, possibly occurring as bertrandite [57]. The higher concentration of Be in the sinters than in the sediments also supported the conclusion that the carbonate minerals have stronger capability to capture Be than other minerals.

Table 4. Minerals in the hot spring sediments and sinters identified by XRD.

Sample	Mineral				
Sediment 1	Calcite, $CaCO_3$	Aragonite, $CaCO_3$	Quartz, SiO_2	Albite, $NaAlSi_3O_8$	/
Sediment 2	Calcite, $CaCO_3$	/	Quartz, SiO_2	Albite, $NaAlSi_3O_8$	/
Sediment 3	Calcite, $CaCO_3$	/	Quartz, SiO_2	Albite, $NaAlSi_3O_8$	Muscovite, $KAl_2Si_3AlO_{10}(OH)_2$
Sediment 4	/	/	Quartz, SiO_2	/	Muscovite, $KAl_2Si_3AlO_{10}(OH,F)_2$
Sediment 5	/	/	Quartz, SiO_2	Albite, $NaAlSi_3O_8$	Muscovite, $(K_{0.82}Na_{0.18})(Fe_{0.03}Al_{1.97})(AlSi_3)O_{10}(OH)_2$
Sediment 6	/	/	Quartz, SiO_2	Albite, $NaAlSi_3O_8$	Muscovite, $KAl_2Si_3AlO_{10}(OH,F)_2$
Sediment 7	Calcite, $CaCO_3$	/	Quartz, SiO_2	Albite, $NaAlSi_3O_8$	Muscovite, $KAl_2Si_3AlO_{10}(OH,F)_2$
Sediment 8	/	/	Quartz, SiO_2	Albite, $NaAlSi_3O_8$	Orthoclase, Ba-rich, $(K,Ba)(Si,Al)_4O_8$
Sediment 9	/	/	Quartz, SiO_2	/	Muscovite, $KAl_2Si_3AlO_{10}(OH)_2$
Sediment 10	Calcite, $CaCO_3$	/	Quartz, SiO_2	Albite, $NaAlSi_3O_8$	Muscovite, $KAl_2Si_3AlO_{10}(OH)_2$
Sediment 11	Calcite, $CaCO_3$	Aragonite, $CaCO_3$	Quartz, SiO_2	/	Muscovite, $KAl_2Si_3AlO_{10}(OH,F)_2$
Sediment 12	Calcite, $CaCO_3$	Aragonite, $CaCO_3$	Quartz, SiO_2	Albite, $NaAlSi_3O_8$	Muscovite, $(K,Na)Al_2(Si,Al)_4O_{10}(OH)_2$
Sinter 1	Calcite, $CaCO_3$	Aragonite, $CaCO_3$	/	/	/
Sinter 2	Calcite, $CaCO_3$	Aragonite, $CaCO_3$	/	/	/
Sinter 3	Calcite, $CaCO_3$	Aragonite, $CaCO_3$	/	/	/

As in the sediments showed positive correlations with the Fe and S contents (**Figure 6**B). In natural environment, the occurrence of As is commonly geochemically controlled by the Fe-bearing phases [59-64]. In the geothermal systems, As can be retained by the hot spring sinter [65]. Although As may be present as arsenate sorbed on hydrous ferric oxides or as nodular arsenide micro-mineralization similar to loellingite ($FeAs_2$) [66], the positive correlations between As, Fe, and S (**Table 3** and **Figure 6**B) suggested that As was probably associated with pyrite because pyrite is often detected in hot spring sediments [54, 67]. Cs in the sediments showed positive correlations with Ca, Mg, Sr and Na (**Figure 6**C), indicating that Cs was probably associated with carbonates and albite. The situation for Tl was similar to As, its concentrations were positively related with Fe, S, and Ba contents.

Similar to the situation of As, Co, Tl, Se, and U also showed positive correlation with Fe and S contents (**Table 5**). Thus, Co, Tl, Se, and U were also possibly associated with Fe sulfides such as pyrite. Clay mineral often play an important role in trace elements retention in nature. V in nature is most possibly associated with clay minerals and pyrite [68]. In clay minerals, V can be adsorbed through surface complexation and electrostatic interaction (Na^+-bridge) [69]. Cr was probably to be adsorbed to mineral surfaces, to form stable surface complexes, surface precipitation and ion exchange in clay minerals [70, 71]. In this study, V and Cr both showed positive relationship with Si and Al (**Table 5**), indicating that they were possibly associated with clay minerals in the sediments. Their positive correlation with K contents further indicated that they might be associated with muscovite

and/or orthoclase. Cu was supposed to be present as sulfide like chalcopyrite according to its positive correlation with S contents.

Table 5. Pearson correlation coefficients between the major and minor elements and the PHEs in the sediments.

	CaO	SiO_2	Al_2O_3	Fe_2O_3	K_2O	Na_2O	MgO	SrO	TiO_2	BaO	SO_3	P_2O_5
Be	**0.85**	-0.77	-0.78	-0.19	-0.83	0.36	**0.91**	**0.89**	-0.77	0.21	-0.29	-0.34
V	-0.57	**0.65**	**0.77**	-0.39	**0.59**	-0.75	-0.48	-0.55	0.24	-0.49	-0.20	-0.08
Cr	-0.69	**0.60**	**0.54**	0.20	**0.55**	-0.59	-0.76	-0.70	0.45	-0.05	0.50	0.25
Mn	-0.16	0.19	0.41	-0.07	0.21	-0.42	-0.05	-0.14	-0.12	-0.27	-0.20	0.06
Co	-0.47	0.30	0.27	**0.52**	0.25	-0.51	-0.57	-0.44	0.06	0.32	**0.70**	0.04
Ni	-0.50	0.39	0.43	0.33	0.34	-0.63	-0.51	-0.46	0.02	0.10	0.47	0.01
Cu	-0.54	0.44	0.35	0.25	0.25	-0.80	-0.62	-0.48	-0.01	0.18	**0.54**	-0.22
Zn	0.27	-0.32	0.12	0.18	-0.11	0.12	0.28	0.23	-0.20	0.04	-0.21	0.36
As	-0.35	0.12	-0.08	**0.75**	-0.06	-0.35	-0.49	-0.30	0.01	**0.65**	**0.92**	-0.10
Se	0.19	-0.36	-0.40	**0.66**	-0.38	0.05	-0.36	0.22	-0.18	**0.83**	**0.53**	0.01
Cd	0.07	-0.19	0.42	0.38	0.14	0.15	-0.24	-0.05	0.35	0.28	-0.03	**0.57**
Cs	**0.79**	-0.78	-0.47	0.08	-0.47	**0.76**	**0.55**	**0.72**	-0.15	0.20	-0.38	0.28
Tl	-0.31	0.10	-0.13	**0.70**	-0.07	-0.31	-0.45	-0.26	0	**0.63**	**0.93**	-0.11
Pb	0.36	-0.43	0.18	0.26	-0.11	0.44	0.19	0.22	0.26	0.22	-0.24	**0.61**
U	-0.33	0.09	0.31	**0.78**	0.18	0.03	-0.54	-0.38	0.49	**0.57**	**0.63**	0.46

Note: Underlined and bold digits represent a positive correlation for 12 determinations ($P < 0.05$).

4. Conclusions

In order to investigate the influence of the mineral deposition on the retention of the PHEs in the geothermal hot spring vents, the hot spring water and the sediments sampled from the Nagqu geothermal field on the Tibetan Plateau were analyzed from the perspective of geochemistry and mineralogy. The results showed that the hot spring water samples did not show highly elevated PHE concentrations. However, in some cases, the concentrations of Be, As, and Tl exceeded the class III groundwater of China up to 2, 2, and 19 times, respectively. This indicated that the hot spring water in the Nagqu geothermal field has a potential to influence the local water system and possibly cause further environmental and health concerns. Cs had a high concentration up to 776 μg/L in the hot spring water samples, which was much higher than the general levels in the common aqueous systems. The relative high concentrations of these elements have impacted the sediments, showing higher concentrations than the background levels of the Tibetan surface soils. The I_{geo} calculation indicated that the sediments were moderately contaminated by Cs and Tl. The XRD results showed that the major mineralogical compositions of hot spring sediments were calcite, quartz, aragonite, albite, muscovite, and orthoclase, while the sinters mainly contained calcite and aragonite. The occurrence of the PHEs in the sediments at the hot spring vents resulted from the retention of various minerals. The correlation analysis between the major and minor elements and the PHEs indicated that the carbonate minerals calcite and aragonite had affinity to Be and Cs. Sulfide minerals such as pyrite were probably the dominant capturer of As and Tl. The Fe-bearing minerals or the Fe sulfides also showed affinity with Co, Se, and U. Clay and feldspar minerals mainly retained V and Cr. The capture of the minerals deposited at the spring vents influenced the immobility of the geothermal source PHEs on Earth's surface.

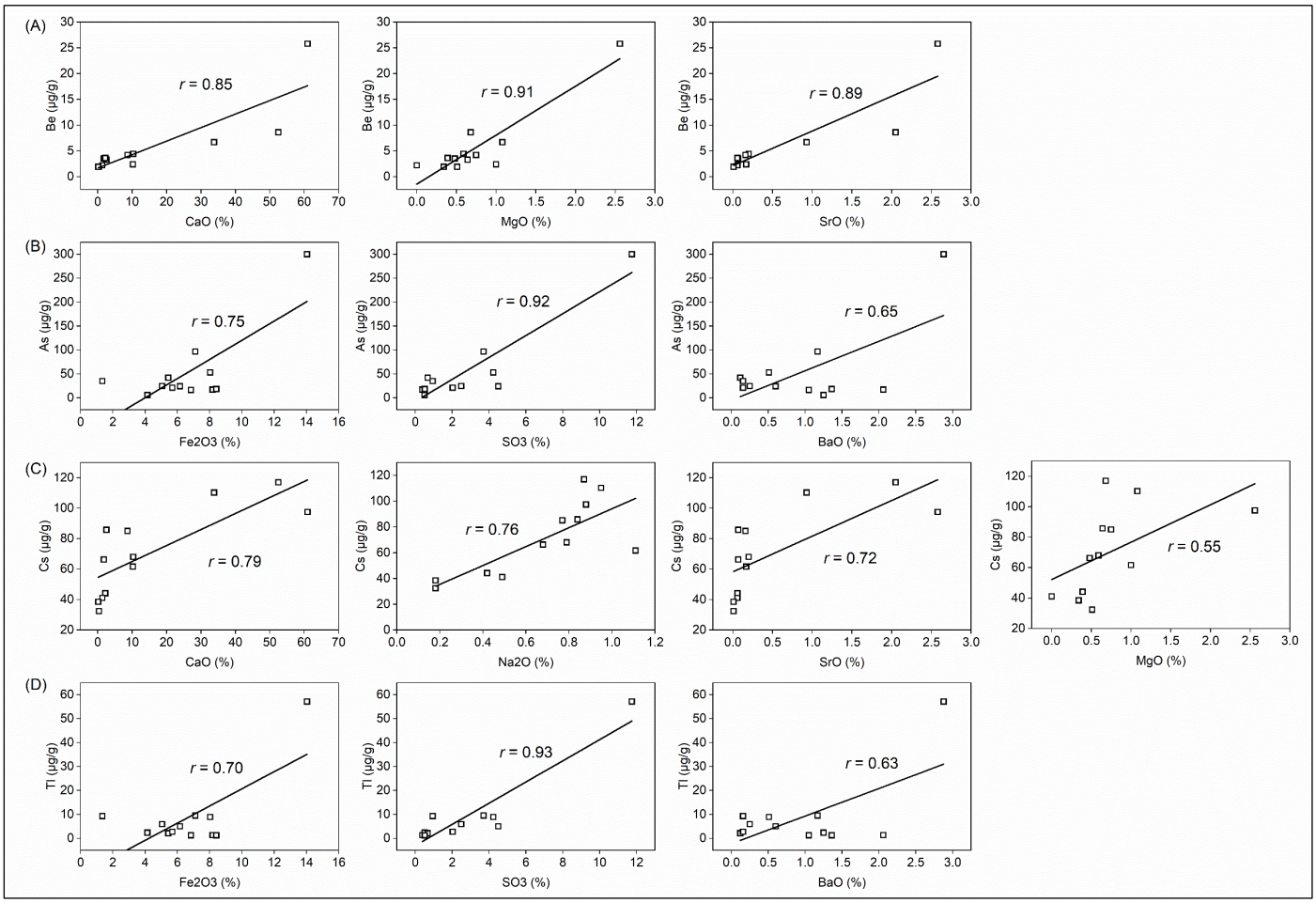

Figure 6. Positive correlations ($r > 0.4973$, $P < 0.05$) between the elevated PHEs and the major and minor elements in the hot spring sediments.

Author Contributions: Conceptualization, Y. W. and H. C.; Methodology, Y. W.; Formal analysis, Y. W.; Investigation, Y. W.; Writing - Original Draft, Y. W. and H. C.; Funding acquisition, H. C.

Funding: This work was supported in parts by the Second Tibetan Plateau Scientific Expedition and Research Program (2019QZKK0605), the Natural Science Foundation of China (Grant Nos. 41877112, 42077110, and 41725015), and the China Postdoctoral Science Foundation (2021M700199).

Data Availability Statement: Data are available on request.

Acknowledgments: In this section, you can acknowledge any support given which is not covered by the author contribution or funding sections. This may include administrative and technical support, or donations in kind (e.g., materials used for experiments).

Conflicts of Interest: The authors declare no conflict of interest.

References

1. Wu, Y.; Zhou, X.; Zhuo, L.; Tao, G.; Ma, J.; Wang, Y., Structural controls of the northern Red River Fault Zone on the intensity of hydrothermal activity and distribution of hot springs in the Yunnan-Tibet geothermal belt. Geothermics 2023, 109, 102641.
2. Guo, Q., Hydrogeochemistry of high-temperature geothermal systems in China: A review. Applied Geochemistry 2012, 27, (10), 1887-1898.

3. Hu, Y.; Cheng, H.; Tao, S., Opportunity and challenges in large-scale geothermal energy exploitation in China. Critical Reviews in Environmental Science and Technology 2022, 52, (21), 3813-3834.
4. Nshimyumuremyi, E.; Junqi, W., Geothermal reservoir heat transfer, temperature modelling and electrical power potential estimation: Gisenyi hot spring. IET Renewable Power Generation 2020, 14, (9), 1463-1470.
5. Hu, Y.; Cheng, H.; Tao, S., Environmental and human health impacts of geothermal exploitation in China and mitigation strategies. Critical Reviews in Environmental Science and Technology 2022, 1-24.
6. Arslan, Ş.; Avşar, Ö., Assessment of heavy metal pollution in Köyceğiz-Dalyan coastal lagoon watershed (Muğla) SW Turkey. Arabian Journal of Geosciences 2020, 13, (15), 719.
7. Vranovská, A.; Bodiš, D.; Sracek, O.; Ženišová, Z., Anomalous arsenic concentrations in the Ďurkov carbonate geothermal structure, eastern Slovakia. Environmental Earth Sciences 2015, 73, (11), 7103-7114.
8. Bernard, R.; Taran, Y.; Pennisi, M.; Tello, E.; Ramirez, A., Chloride and Boron behavior in fluids of Los Humeros geothermal field (Mexico): A model based on the existence of deep acid brine. Applied Geochemistry 2011, 26, (12), 2064-2073.
9. Baba, A.; Uzelli, T.; Sozbilir, H., Distribution of geothermal arsenic in relation to geothermal play types: A global review and case study from the Anatolian plate (Turkey). Journal of Hazardous Materials 2021, 414, 125510.
10. Moeck, I. S., Catalog of geothermal play types based on geologic controls. Renewable and Sustainable Energy Reviews 2014, 37, 867-882.
11. Morales-Arredondo, J. I.; Esteller-Alberich, M. V.; Armienta Hernández, M. A.; Martínez-Florentino, T. A. K., Characterizing the hydrogeochemistry of two low-temperature thermal systems in Central Mexico. Journal of Geochemical Exploration 2018, 185, 93-104.
12. Birkle, P.; Bundschuh, J.; Sracek, O., Mechanisms of arsenic enrichment in geothermal and petroleum reservoirs fluids in Mexico. Water Research 2010, 44, (19), 5605-5617.
13. Durowoju, O. S.; Odiyo, J. O.; Ekosse, G.-I. E., Variations of Heavy Metals from Geothermal Spring to Surrounding Soil and Mangifera Indica–Siloam Village, Limpopo Province. In Sustainability, 2016; Vol. 8.
14. Yang, G. F.; Wang, D. L.; Li, N.; Zhuo, S. G., The Distribution and Environment Problems of Geothermal Springs in Development and Utilization in Beijing-Tianjin-Tangshan-Qinhuangdao Area, China. Applied Mechanics and Materials 2013, 295-298, 1948-1951.
15. Guo, Q.; Wang, Y., Trace Element Hydrochemistry Indicating Water Contamination in and Around the Yangbajing Geothermal Field, Tibet, China. Bulletin of Environmental Contamination and Toxicology 2009, 83, (4), 608-613.
16. Guo, Q.; Wang, Y.; Liu, W., Hydrogeochemistry and environmental impact of geothermal waters from Yangyi of Tibet, China. Journal of Volcanology and Geothermal Research 2009, 180, (1), 9-20.
17. Guo, Q.; Wang, Y.; Liu, W., B, As, and F contamination of river water due to wastewater discharge of the Yangbajing geothermal power plant, Tibet, China. Environmental Geology 2008, 56, (1), 197-205.
18. Rehman, K.; Fatima, F.; Waheed, I.; Akash, M. S. H., Prevalence of exposure of heavy metals and their impact on health consequences. Journal of Cellular Biochemistry 2018, 119, (1), 157-184.
19. Yang, Q.; Li, Z.; Lu, X.; Duan, Q.; Huang, L.; Bi, J., A review of soil heavy metal pollution from industrial and agricultural regions in China: Pollution and risk assessment. Science of The Total Environment 2018, 642, 690-700.
20. Li, Z.; Ma, Z.; van der Kuijp, T. J.; Yuan, Z.; Huang, L., A review of soil heavy metal pollution from mines in China: Pollution and health risk assessment. Science of The Total Environment 2014, 468-469, 843-853.
21. Beckers, F.; Rinklebe, J., Cycling of mercury in the environment: Sources, fate, and human health implications: A review. Critical Reviews in Environmental Science and Technology 2017, 47, (9), 693-794.
22. Ali, H.; Khan, E.; Ilahi, I., Environmental Chemistry and Ecotoxicology of Hazardous Heavy Metals: Environmental Persistence, Toxicity, and Bioaccumulation. Journal of Chemistry 2019, 2019, 6730305.

23. Varekamp, J. C., The volcanic acidification of glacial Lake Caviahue, Province of Neuquen, Argentina. Journal of Volcanology and Geothermal Research 2008, 178, (2), 184-196.
24. Ng, J. C.; Wang, J.; Shraim, A., A global health problem caused by arsenic from natural sources. Chemosphere 2003, 52, (9), 1353-1359.
25. Sunguti, A. E.; Kinyanjui, T. K. J. J. o. N., A review of the status of organic pollutants in geothermal waters. 2021, 4, 19-28.
26. Fournier, R. O.; Rowe, J. J., Estimation of underground temperatures from the silica content of water from hot springs and wet-steam wells. Advanced topics in information engineering /: 1966.
27. Boudreau, A. E.; Lynne, B. Y., The growth of siliceous sinter deposits around high-temperature eruptive hot springs. Journal of Volcanology and Geothermal Research 2012, 247-248, 1-8.
28. Jones, B., Review of aragonite and calcite crystal morphogenesis in thermal spring systems. Sedimentary Geology 2017, 354, 9-23.
29. Shiraishi, F.; Morikawa, A.; Kuroshima, K.; Amekawa, S.; Yu, T.-L.; Shen, C.-C.; Kakizaki, Y.; Kano, A.; Asada, J.; Bahniuk, A. M., Genesis and diagenesis of travertine, Futamata hot spring, Japan. Sedimentary Geology 2020, 405, 105706.
30. Liu, H.; Zhou, X.; Zhang, Y.; Wang, M.; Tan, M.; Hai, K.; Yu, M.; Huo, D., Hydrochemical characteristics of travertine-depositing hot springs in western of Yunnan, China. Quaternary International 2020, 547, 63-74.
31. Luo, L.; Capezzuoli, E.; Rogerson, M.; Vaselli, O.; Wen, H.; Lu, Z., Precipitation of carbonate minerals in travertine-depositing hot springs: Driving forces, microenvironments, and mechanisms. Sedimentary Geology 2022, 438, 106207.
32. Campbell, K. A.; Guido, D. M.; Gautret, P.; Foucher, F.; Ramboz, C.; Westall, F., Geyserite in hot-spring siliceous sinter: Window on Earth's hottest terrestrial (paleo)environment and its extreme life. Earth-Science Reviews 2015, 148, 44-64.
33. Ünal Ercan, H.; Işık Ece, Ö.; Schroeder, P. A.; Gülmez, F., Characteristics and evolution of the Etili silica sinter epithermal deposits, Çanakkale – Turkey: Relation to alkali chloride vs acid-sulfate fluids. Ore Geology Reviews 2022, 142, 104726.
34. Zhao, Q.; Guo, Q.; Luo, L.; Yan, K., Tungsten Accumulation in Hot Spring Sediments Resulting from Preferred Sorption of Aqueous Polytungstates to Goethite. In International Journal of Environmental Research and Public Health, 2021; Vol. 18.
35. Leal-Acosta, M. L.; Shumilin, E.; Mirlean, N.; Sapozhnikov, D.; Gordeev, V., Arsenic and Mercury Contamination of Sediments of Geothermal Springs, Mangrove Lagoon and the Santispac Bight, Bahía Concepción, Baja California Peninsula. Bulletin of Environmental Contamination and Toxicology 2010, 85, (6), 609-613.
36. Zhang, G.; Liu, C.-Q.; Liu, H.; Jin, Z.; Han, G.; Li, L., Geochemistry of the Rehai and Ruidian geothermal waters, Yunnan Province, China. Geothermics 2008, 37, (1), 73-83.
37. Guo, Q.; Li, Y.; Luo, L., Tungsten from typical magmatic hydrothermal systems in China and its environmental transport. Science of The Total Environment 2019, 657, 1523-1534.
38. Cumbal, L.; Vallejo, P.; Rodriguez, B.; Lopez, D., Arsenic in geothermal sources at the north-central Andean region of Ecuador: concentrations and mechanisms of mobility. Environmental Earth Sciences 2010, 61, (2), 299-310.
39. Guo, Q.; Planer-Friedrich, B.; Luo, L.; Liu, M.; Wu, G.; Li, Y.; Zhao, Q., Speciation of antimony in representative sulfidic hot springs in the YST Geothermal Province (China) and its immobilization by spring sediments. Environmental Pollution 2020, 266, 115221.
40. Li, C.; Kang, S.; Chen, P.; Zhang, Q.; Mi, J.; Gao, S.; Sillanpää, M., Geothermal spring causes arsenic contamination in river waters of the southern Tibetan Plateau, China. Environmental Earth Sciences 2014, 71, (9), 4143-4148.
41. Xu, P.; Tan, H.; Zhang, Y.; Zhang, W., Geochemical characteristics and source mechanism of geothermal water in Tethys Himalaya belt (in Chinese with English abstract). Geology in China 2018, 45, (6), 13.
42. Guo, Q.; Planer-Friedrich, B.; Liu, M.; Yan, K.; Wu, G., Magmatic fluid input explaining the geochemical anomaly of very high arsenic in some southern Tibetan geothermal waters. Chemical Geology 2019, 513, 32-43.

43. Guo, L.; Wang, G.; Sheng, Y.; Sun, X.; Shi, Z.; Xu, Q.; Mu, W., Temperature governs the distribution of hot spring microbial community in three hydrothermal fields, Eastern Tibetan Plateau Geothermal Belt, Western China. Science of The Total Environment 2020, 720, 137574.
44. Wang, X.; Yin, Y.; Yu, Z.; Shen, G.; Cheng, H.; Tao, S., Distinct distribution patterns of the abundant and rare bacteria in high plateau hot spring sediments. Science of The Total Environment 2023, 863, 160832.
45. Mathurin, F. A.; Drake, H.; Tullborg, E.-L.; Berger, T.; Peltola, P.; Kalinowski, B. E.; Åström, M. E., High cesium concentrations in groundwater in the upper 1.2km of fractured crystalline rock – Influence of groundwater origin and secondary minerals. Geochimica et Cosmochimica Acta 2014, 132, 187-213.
46. Nakaya, S.; Phan, H. M. H.; Iwai, Y.; Itoh, A.; Aoki, H.; Nakano, T., Longtime behavior of cesium (Cs) in natural spring drinking water. Sustainability of Water Quality and Ecology 2015, 6, 20-30.
47. Administration), C. C. N. E. P.; Centre), C. C. N. E. M., Background values of elements in Chinese soil (in Chinese). China Environmental Science Press: 1990.
48. Muller, G., Index of geo-accumulation in sediments of the Rhine river. GeoJournal 1969, 2, (3), 109-118.
49. Colman, D. R.; Feyhl-Buska, J.; Robinson, K. J.; Fecteau, K. M.; Xu, H.; Shock, E. L.; Boyd, E. S., Ecological differentiation in planktonic and sediment-associated chemotrophic microbial populations in Yellowstone hot springs. FEMS Microbiology Ecology 2016, 92, (9), fiw137.
50. Pentecost, A., Travertine. Springer, Berlin: 2005.
51. Jones, B.; Renaut, R. W., Chapter 4 Calcareous Spring Deposits in Continental Settings. In Developments in Sedimentology, Alonso-Zarza, A. M.; Tanner, L. H., Eds. Elsevier: 2010; Vol. 61, pp 177-224.
52. Capezzuoli, E.; Gandin, A.; Pedley, M., Decoding tufa and travertine (fresh water carbonates) in the sedimentary record: The state of the art. Sedimentology 2014, 61, (1), 1-21.
53. Kano, A.; Okumura, T.; Takashima, C.; Shiraishi, F., Geomicrobiological Properties and Processes of Travertine. Springer, Singapore: 2019.
54. Landa-Arreguín, J. F. A.; Villanueva-Estrada, R. E.; Rodríguez-Díaz, A. A.; Morales-Arredondo, J. I.; Rocha-Miller, R.; Alfonso, P., Evidence of a new geothermal prospect in the Northern-Central trans-Mexican volcanic belt: Rancho Nuevo, Guanajuato, Mexico. Journal of Iberian Geology 2021, 47, (4), 713-732.
55. Geptner, A.; Kristmannsdóttir, H.; Kristjansson, J.; Marteinsson, V., Biogenic saponite from an active submarine hot spring, Iceland. Clays and Clay Minerals 2002, 50, (2), 174-185.
56. Luan, G.; Wang, W.; Liu, D.; Liu, J., The eruptive flow sediments in Jimo warm spring of Qingdao and its depositional model (In Chinese with English abstract). ACTA GEOSCIENCE SINICA 2003, 24, (4), 357-360.
57. Foley, N. K.; Hofstra, A. H.; Lindsey, D. A.; Seal Ii, R. R.; Jaskula, B. W.; Piatak, N. M. Occurrence model for volcanogenic beryllium deposits; 2010-5070F; Reston, VA, 2012; p 52.
58. Pisarskii, B. I.; Konev, A. A.; Levi, K. G.; Delvaux, D., CARBON DIOXIDE-BEARINGALKALINE HYDROTHERMS AND STRONTIUM-BEARINGTRAVERTINES IN THE SONGWE RIVER VALLEY (Tanzania). Russian Geology and Geophysics 1998, 39, (7), 941-948.
59. Stolze, L.; Battistel, M.; Rolle, M., Oxidative Dissolution of Arsenic-Bearing Sulfide Minerals in Groundwater: Impact of Hydrochemical and Hydrodynamic Conditions on Arsenic Release and Surface Evolution. Environmental Science & Technology 2022, 56, (8), 5049-5061.
60. Qiao, W.; Guo, H.; He, C.; Shi, Q.; Xing, S.; Gao, Z., Identification of processes mobilizing organic molecules and arsenic in geothermal confined groundwater from Pliocene aquifers. Water Research 2021, 198, 117140.
61. Cheng, H.; Hu, Y.; Luo, J.; Xu, B.; Zhao, J., Geochemical processes controlling fate and transport of arsenic in acid mine drainage (AMD) and natural systems. Journal of Hazardous Materials 2009, 165, (1), 13-26.

62. Garcia-Rios, M.; De Windt, L.; Luquot, L.; Casiot, C., Modeling of microbial kinetics and mass transfer in bioreactors simulating the natural attenuation of arsenic and iron in acid mine drainage. Journal of Hazardous Materials 2021, 405, 124133.
63. Park, J. H.; Han, Y.-S.; Ahn, J. S., Comparison of arsenic co-precipitation and adsorption by iron minerals and the mechanism of arsenic natural attenuation in a mine stream. Water Research 2016, 106, 295-303.
64. Rango, T.; Vengosh, A.; Dwyer, G.; Bianchini, G., Mobilization of arsenic and other naturally occurring contaminants in groundwater of the Main Ethiopian Rift aquifers. Water Research 2013, 47, (15), 5801-5818.
65. Villalba, E.; Tanjal, C.; Borzi, G.; Páez, G.; Carol, E., Geogenic arsenic contamination of wet-meadows associated with a geothermal system in an arid region and its relevance for drinking water. Science of The Total Environment 2020, 720, 137571.
66. Alsina, M. A.; Zanella, L.; Hoel, C.; Pizarro, G. E.; Gaillard, J.-F.; Pasten, P. A., Arsenic speciation in sinter mineralization from a hydrothermal channel of El Tatio geothermal field, Chile. Journal of Hydrology 2014, 518, 434-446.
67. Dutta, A.; Mishra, P.; Absar, A.; Malviya, V. P.; Singh, P. K.; Srivastava, A.; Ray, B.; Kumar, A.; Nitnaware, N. V., Tracing hydrothermal mineral thenardite in geysers/hot springs of North-western Himalayan belt, Ladakh Geothermal Province, India by hydrogeochemistry, fluid-mineral equilibria and isotopic studies. Geochemistry 2023, 125973.
68. Awan, R. S.; Liu, C.; Yang, S.; Wu, Y.; Zang, Q.; Khan, A.; Li, G., The occurrence of vanadium in nature: its biogeochemical cycling and relationship with organic matter—a case study of the Early Cambrian black rocks of the Niutitang Formation, western Hunan, China. Acta Geochimica 2021, 40, (6), 973-997.
69. Zhu, H.; Xiao, X.; Guo, Z.; Han, X.; Liang, Y.; Zhang, Y.; Zhou, C., Adsorption of vanadium (V) on natural kaolinite and montmorillonite: Characteristics and mechanism. Applied Clay Science 2018, 161, 310-316.
70. Taghipour, M.; Jalali, M., Effect of clay minerals and nanoparticles on chromium fractionation in soil contaminated with leather factory waste. Journal of Hazardous Materials 2015, 297, 127-133.
71. Joe-Wong, C.; Brown, G. E., Jr.; Maher, K., Kinetics and Products of Chromium(VI) Reduction by Iron(II/III)-Bearing Clay Minerals. Environmental Science & Technology 2017, 51, (17), 9817-9825.